Either the absence of suitable hosts or the inhibition of host-seeking by harsh climatic conditions would make autogeny the only means for population survival. In the variable and at times severe climatic regions of the temperate and arctic zones, both of these factors definitely appear to be major forces selecting for autogeny (*8, 9*).

The present report is the first to describe a distribution where the capacity to produce autogenous eggs increases from northern to southern populations. Little is known concerning the relative influence of specific environmental factors on the occurrence of autogeny in field populations of *A. taeniorhynchus*. Yet preliminary evidence indicates that even in this species host scarcity might be an important factor selecting for autogeny. For example, Edman (*10*) recently found that in east-central Florida *A. taeniorhynchus* feeds primarily on mammals. More than 80 percent of the identified blood meals were from rabbits and ruminants. Neither type of mammalian host was abundant in the immediate coastal areas of this region, and blood engorgement rates were very low, but 8 miles (13 km) inland suitable hosts were more numerous and blood engorgement rates were three times higher (*10*). There is a definite need for additional studies on mosquito-host interrelations. Such studies would certainly improve our understanding of the influence of host abundance on the frequency and expression of autogeny in *A. taeniorhynchus*.

GEORGE F. O'MEARA
DAVID G. EVANS
Entomological Research Center,
Post Office Box 520,
Vero Beach, Florida 32960

References and Notes

1. J. A. Downes, *Annu. Rev. Entomol.* **10**, 257 (1965).
2. ———, *Proc. 10th Int. Congr. Entomol.* **3**, 801 (1958).
3. J. F. Anderson, *Ann. Entomol. Soc. Amer.* **64**, 1421 (1971).
4. A. Spielman, *Annu. Rev. Entomol.* **16**, 231 (1971).
5. G. F. O'Meara and G. B. Craig, Jr., *Ann. Entomol. Soc. Amer.* **63**, 1392 (1970).
6. Aquatic stages were reared in enamel pans which contained 350 ml of water and 80 larvae. Synchronous larval development in 6 days was achieved with the use of a diet composed of 1 part powdered brewers' yeast, 1 part lactalbumin, and 1 part pulverized Lab Chow. This mixture was put in each pan according to the following schedule: day 1, 1 unit; day 2, 1 unit; day 3, 3 units; day 4, 4 units; day 5, 4 units (1 unit equals 50 mg). Upon emergence, females were isolated in glass vials and allowed to feed ad libitum on 10 percent sugar solution. Ovarian examinations were performed on females which were at least 5 days old. Only development to stage V was classified as autogenous. For a description of mosquito ovarian stages, see S. R. Christophers [*Paludism* **2**, 73 (1911)].
7. A. Spielman, *Amer. J. Hyg.* **80**, 175 (1964).
8. P. S. Corbet, *Nature* **203**, 669 (1964); *ibid.* **215**, 662 (1967).
9. H. C. Berg and D. A. Brown, *ibid.* **239**, 500
10. J. D. Edman, *ibid.*, p. 687.
11. We thank C. W. Lee, W. J. Crans, and F. Lesser for sending us mosquitoes. This investigation was supported in part by research grant No. AI-11583 and general support grant No. FR-05553 from NIH.

19 March 1973

Dynamics of Number Fluctuations: Motile Microorganisms

Abstract. *The time dependence of the intensity of light scattered from motile* Escherichia coli *bacteria is studied in population densities so low that the intensity autocorrelation function reflects fluctuations in the total number of particles in the scattering region. Measured correlation functions are analyzed by using a random walk model of bacterial motion.*

It has recently become apparent that important information on the dynamic properties of microscopic particles can be obtained by study of the time dependence of the fluctuating intensity of light scattered from systems in which the total number of particles varies with time (*1*). When $\langle N \rangle$, the average number of particles in the illuminated scattering region, is of order unity, a very slowly decaying mode appears in the intensity correlation function, due to fluctuations in the total number of scatterers in the scattering volume (occupation number fluctuations). The characteristic time of this mode reflects the residence time of a typical particle in the scattering region. In this report, experimental data are presented on the dynamics of occupation number fluctuations for motile (swimming) microorganisms. These data are interpreted by using a random walk model of particle motion.

The work reported here represents a useful biological application of a very general method. Although the most promising application of this method is in the area of chemotaxis and phototaxis, fluctuations due to chemical reactions (*2*) and turbulence can be studied by analogous techniques. In fact, these methods apply whenever the number of particles under study is small (say less than 20), or their relative positions are correlated over distances of the order of 1 μm, or both.

Although modern photon counting techniques are employed here, the experiments could in principle have been performed by a patient observer equipped with only a microscope. The observer would record (at half-second intervals) the number of bacteria appearing in a well-defined volume. In the work reported here, the measurement of scattered light intensity merely provides a convenient way to "count" particles.

The total field scattered at time t by a system of M identical, isotropic particles is proportional to a properly weighted sum of the phase factors introduced by each particle,

$$E(K,t) = \sum_{j=1}^{M} \mathcal{E}(\mathbf{r}_j) \exp\,[i\mathbf{K}\cdot\mathbf{r}_j(t)] \quad (1)$$

where $\mathbf{r}_j$ is the position of particle j, $\mathcal{E}(\mathbf{r})$ is the amplitude of the field scattered by a particle when at position $\mathbf{r}$, i is the imaginary unit, and $\mathbf{K}$ is the scattering vector. For incident light of wave vector $\mathbf{K}_0$, $K = 2K_0 \sin\,(\theta/2)$, θ being the scattering angle and K and K_0 the magnitudes of the vectors $\mathbf{K}$ and $\mathbf{K}_0$. In the experiments reported here, the scattering region is defined in two dimensions (x,y) by a focused laser beam and in the third dimension (z) by a narrow collection slit. For this configuration, $\mathcal{E}(\mathbf{r})$ can be represented by

$$\mathcal{E}(\mathbf{r}) \propto \exp\{[-(x^2 + y^2)/\sigma_1^2] - z^2/\sigma_2^2\} \quad (2)$$

where σ_1 and σ_2 are the points where the intensity profile of the incident beam and the transmission profile of the slit are $1/e^2$ of their initial values. Diffraction at the slit produces the approximate Gaussian profile in the z direction.

Since the scattered intensity $I(t)$ is proportional to $|E(t)|^2$, the correlation function $\langle I(0)I(t)\rangle$ of the scattered intensity follows directly from Eq. 1. If $K^{-1} \ll (\sigma_1,\sigma_2)$,

$$\langle I(0)I(t)\rangle \propto \langle N\rangle^2 + \langle N\rangle^2|F(K,t)|^2 + \langle \delta N(0)\delta N(t)\rangle \quad (3a)$$

$$\langle \delta N(0)\delta N(t)\rangle = \rho \int\int d\mathbf{r}_1 d\mathbf{r}_2 \mathcal{E}^2(\mathbf{r}_1)\,\mathcal{E}^2(\mathbf{r}_2)\,p(\mathbf{r}_2 - \mathbf{r}_1;t) \quad (3b)$$

where ρ is the number density of scatterers and $\langle N\rangle = \pi^{3/2}\sigma_1^2\sigma_2\rho$ is the average number of particles in the scat-

tering region; $p(\mathbf{r}_2 - \mathbf{r}_1;t)$ is the probability that a particle will be observed at $\mathbf{r}_2$ at time t if that particle was at $\mathbf{r}_1$ at time 0; and $F(K,t)$ is the self-intermediate scattering function (*3*). The characteristic decay time of $|F(K,t)|$ is roughly the time it takes a particle to move a distance $1/K$, typically milliseconds. Although $F(K,t)$ is not of central importance to this work, the mean squared swimming speed was determined from the initial decay of $|F(K,t)|$.

The final term of Eq. 3 is the occupation number correlation function $\langle \delta N(0)\,\delta N(t)\rangle$, the object of this study. This function, which is a generalization of the probability after-effect function (*4*), makes a significant contribution to $\langle I(0)I(t)\rangle$ only if $\langle (\delta N)^2\rangle = \langle N\rangle$, the mean squared fluctuation in the number of particles, is comparable to $\langle N\rangle^2$. The characteristic time of $\langle \delta N(0)\,\delta N(t)\rangle$ is the time required for a typical particle to move distances of the order of (σ_1,σ_2) (*1*).

Calculation of $\langle \delta N(0)\,\delta N(t)\rangle$ requires the specification of a model of the particle motion. For example, if the displacement of the scattering centers is Gaussian with a zero mean (*4*),

$$\langle \delta N(0)\delta N(t)\rangle = \frac{\langle N\rangle \sigma_1^2}{\sigma_1^2 + w(t)} \times \left[\frac{\sigma_2^2}{\sigma_2^2 + w(t)}\right]^{1/2} \quad (4)$$

where $w(t) = 2\langle (\mathbf{r}_2 - \mathbf{r}_1)^2\rangle/3$. Equation 4 would apply to a thermally diffusing particle (such as nonswimming bacteria) with $w(t) = 4Dt$, D being the self-diffusion constant. An expression similar to Eq. 4 has been derived by Magde *et al.* (*2*) in connection with fluorescence fluctuation experiments.

The opposite extreme from the diffusion model is a free (collisionless) particle model. If $\sigma_2 < \sigma_1$ and the scattering centers move in random directions with uniform speed v,

$$\langle \delta N(0)\delta N(t)\rangle = \frac{\langle N\rangle \pi^{1/2}}{2vt(\sigma_2^{-2} - \sigma_1^{-2})^{1/2}} \times \exp(-v^2t^2/\sigma_1^2)\ \mathrm{erf}[vt(\sigma_2^{-2} - \sigma_1^{-2})^{1/2}] \quad (5)$$

where erf is the error function. Equation 5 would apply to bacteria which swim in straight lines with a single speed v for distances that are long compared to the dimensions of the scattering volume.

Intermediate between the diffusion model and the free particle model is the random walk model. If the particles execute a random walk of step length L, then $\langle \delta N(0)\,\delta N(t)\rangle$ will be sensitive to $\langle L\rangle$, the mean free path, if $\langle L\rangle \approx (\sigma_1,\sigma_2)$. An approximate result for the intermediate case can be obtained by interpolation between calculable limits. For example, if the particles "walk" with a uniform step length L and a velocity v, making random angles between steps, then Eq. 5 applies for $t < L/2v$, whereas Eq. 4 applies for $t > 6L/v$ [the displacement is approximately Gaussian after six steps (*4*)] with $w(t) = 2vL/3$. Thus, within the assumptions of this model, $\langle L\rangle$ can be determined by comparing the measured correlation functions with the interpolated theory. This method not only allows an approximate characterization of bacterial motion, but also provides the framework for a study of the response of the bacteria to environmental stimuli such as chemotactic agents (*5*).

The experimental work consisted of measuring the correlation function of light scattered from dilute suspensions of *Escherichia coli* bacteria. The experiments demonstrate that the motion of motile bacteria is of the random walk type in nature, whereas the motion of nonmotile bacteria is diffusional.

Whenever $\langle \delta N(0)\,\delta N(t)\rangle$ makes a significant contribution to Eq. 3, the amplitude distribution of $E(t)$ is non-Gaussian (*6*). For this reason the "scaled" rather than the more familiar "clipped" photocount correlation function was measured. Koppel and Schaefer (*7*) have demonstrated that a properly scaled function is proportional to $\langle I(0)I(t)\rangle$ regardless of the field statistics.

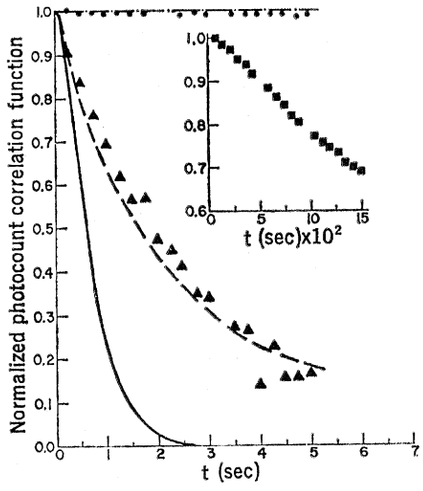

Fig. 1. Scaled photocount correlation function for motile (triangles and squares) and nonmotile (circles) *E. coli* bacteria. The time-independent background has been subtracted and the data are normalized to unity at $t \to 0$. The scattering angles are 15° (squares) and 90° (triangles and circles). Solid curve, calculated curve for a free particle. Dot-dash curve, calculated curve for diffusive motion. Dashed curve, approximate curve for random walk motion. The parameters used for the theoretical curves are $\langle v^2\rangle^{1/2} = 39$ μm/sec, $\langle L\rangle = 17$ μm, $\sigma_1 = 56$ μm, $\sigma_2 = 15.5$ μm, and $D = 4 \times 10^{-9}$ cm²/sec.

Bacterial samples consisted of wild-type *E. coli* K12 grown overnight on L-broth without aeration (*3*). Three drops of the resulting suspension were then diluted into 3 cm³ of 0.01*M* glycerol in 0.01*M* phosphate buffer at *p*H 7. The solution also contained 0.0001*M* ethylenediaminetetraacetic acid, 0.0001*M* 1-methionine, 0.001*M* $(NH_4)_2\,SO_4$, and 0.001*M* $MgSO_4$. The scattering cells were tightly stoppered and data were taken 1 to 2 hours later. Care was exercised to avoid subjecting the bacteria to mechanical disturbance.

The experimental apparatus consisted of a He-Ne laser focused on the center of a cuvette (1 cm by 1 cm) contained in a thermostat (± 0.01°C) at 23.9°C. The collection optics consisted of a lens, a slit, and a photomultiplier. The scaled photocount correlation function was computed on a digital correlator similar to that described by Foord *et al.* (*8*). The scaling circuitry preceded the clipped-at-zero correlator, and scaling levels were high enough that essentially every scaled count was processed.

The parameters σ were measured from the Gaussian curve which best fit the observed $\langle \delta N(0)\,\delta N(t)\rangle$ for suspensions of polystyrene spheres (2 μm in diameter) under uniform translational motion perpendicular (σ_1) and parallel (σ_2) to the incident beam (*7*).

Figure 1 displays the measured correlation function for motile bacteria. Data are also shown for the same solution after 36 hours, when all swimming motion had ceased and the bacteria behaved as Brownian particles. In all cases displayed, the measured time-independent background (first term of Eq. 3) has been subtracted and the curves are normalized to unity at $t \to 0$. In the time range 0.5 to 5 seconds, the second term of Eq. 3 is negligible.

The inset of Fig. 1 shows the measured correlation function at a scattering angle of 15° for the time range 0 to 15 msec. This curve was taken with $\langle N\rangle \geqq 50$ so that the third term of Eq. 3 is negligible. The background has been subtracted so that the resulting curve is just $|F(K,t)|^2$. The average value of v^2 was determined by fitting the initial decay of this curve to $(1 - \langle v^2\rangle t^2K^2/3)$ with the result $\langle v^2\rangle^{1/2} = 39$ μm/sec. The entire speed distribution could not be extracted from $F(K,t)$ by

the method described by Nossal *et al.* (*3*), apparently because of a "wobble" component to the motion in the bacteria.

Three theoretical curves are displayed in Fig. 1. The upper curve is the calculated occupation number correlation function for a Brownian particle with a value of D appropriate for a particle 1 μm in diameter. No decay is visible over the time range covered by Fig. 1. The solid curve is that of a free particle. A comparison of the data with these curves indicates that while nonswimming bacteria behave as Brownian particles, the motile bacteria behave as neither diffusing nor free particles. The broken curve in Fig. 1 is that obtained from the interpolation procedure described above, assuming $\langle v^2 \rangle^{1/2} = 39$ μm/sec and $\langle L \rangle = 17$ μm. Although this curve falls outside the experimental scatter at some points, it must be realized that the assumed δ-function distributions for speed and step length and random angle distribution are a compromise with reality. Nossal *et al.* (*3*), for example, found a strongly skewed velocity distribution, and the data of Berg and Brown (*9*) suggest an exponential step distribution. In addition, Berg and Brown indicate that the angle between steps is not random, but steps are skewed toward small angles. The inclusion of more realistic velocity, step, and angle distributions would complicate the interpretation of the data considerably. Fortunately, however, inclusion of the skewed velocity distribution would result in a longer measured mean free path, while more realistic step-length and angle distributions would imply shorter $\langle L \rangle$. These effects thus tend to cancel, lending validity to the mean free path of 17 μm reported here.

DALE W. SCHAEFER*
IBM T. J. Watson Research Center, Yorktown Heights, New York 10598

References and Notes

1. D. W. Schaefer and B. J. Berne, *Phys. Rev. Lett.* **28**, 475 (1972).
2. D. Magde, E. Elson, W. W. Webb, *ibid.* **29**, 705 (1972).
3. R. Nossal, S.-H. Chen, C.-C. Lai, *Opt. Commun.* **4**, 35 (1971).
4. S. Chandrasekhar, *Rev. Mod. Phys.* **15**, 1 (1943).
5. J. Adler, *Science* **153**, 708 (1966); *ibid.* **166**, 1588 (1969).
6. D. W. Schaefer and P. N. Pusey, *Phys. Rev. Lett.* **29**, 843 (1972).
7. D. E. Koppel and D. W. Schaefer, *Appl. Phys. Lett.* **22**, 36 (1973).
8. R. Foord, E. Jakeman, C. J. Oliver, E. R. Pike, R. J. Blagrove, E. Wood, A. R. Peacocke, *Nature* **227**, 242 (1970).
9. H. C. Berg and D. A. Brown, *ibid.* **239**, 500 (1972).
10. I thank B. J. Berne, N. Friedman, S. H. Koenig, D. E. Koppel, D. Littman, R. Nossal, and P. N. Pusey for helpful suggestions and discussions.
* Present address: Sandia Laboratories, Albuquerque, New Mexico 87115.

18 December 1972; revised 12 March 1973

Axonal Transport of Dopamine-β-Hydroxylase by Human Sural Nerves in vitro

Abstract. *Dopamine-β-hydroxylase activity accumulated above a ligature on biopsy samples of normal human sural nerves incubated in vitro. The rate of accumulation indicated that this enzyme was transported distally at a velocity of 2 millimeters per hour. Axoplasmic transport of dopamine-β-hydroxylase was greatly reduced in sural nerves from a few patients with peripheral neuropathies.*

For many years it has been known that peripheral nerves can transport proteins down their axons at rates of a few millimeters per day (*1*). Recently, it has been discovered that certain proteins flow distally at much higher rates of several millimeters per hour (*2*). The question of how nerves are able to move substances from cell body to terminal regions has attracted much attention. Less well explored is the role of axonal transport in maintaining neuronal structure or function. In this study of human sural nerves in vitro, we have examined transport of dopamine-β-hydroxylase (DBH), the enzyme that catalyzes the final stage in the biosynthesis of norepinephrine (*3*). We undertook these experiments with the aim of characterizing axonal transport of DBH well enough in normal nerves to permit meaningful analysis of the role of transport in disease of peripheral neurons. Results obtained with normal nerves are reported here along with initial observations that point to abnormalities of transport in certain kinds of neuropathy.

As part of an ongoing study of the histology and biochemistry of peripheral nerves, a fascicular biopsy of sural nerve, 3 to 5 cm in length, was obtained at ankle level with informed consent from ten healthy human volunteers, ages 21 to 28 (*4*). The biopsy specimen was about one-third of the thickness of the nerve and had no fascicles entering or leaving. One milliliter of lidocaine (0.75 percent) was instilled directly into the nerve about 2 cm above the site of transection. An oblique cut marked the distal end of the specimen. The nerve was moistened with isotonic saline solution while the epineurium was trimmed off under a dissection microscope. The nerve was then blotted, weighed, and transferred to a beaker containing 200 ml of a bicarbonate-buffered physiological salt solution (*5*). This solution was maintained at 37°C and continuously gassed with 95 percent O_2, 5 percent CO_2; its *p*H was constant at 7.4. After 15 minutes of incubation in this solution, the nerve was ligated with silk thread at the proximal end (ligature 1), at a point about 9 mm from the distal end (ligature 2), and at the distal end (ligature 3). After a further incubation for a variable period of time, the nerve was removed and cut into 3-mm segments which were individually homogenized in glass homogenizers containing 0.6 ml of ice-cold buffer (0.005*M* tris, *p*H 7.4; bovine serum albumin, 0.2 percent; and Triton X-100, 0.1 percent). Homogenates were centrifuged at 15,000*g* for 10 minutes. The supernatant fractions were assayed for DBH activity in 200-μl aliquots with tyramine as a substrate, according to a previously described method (*6*). Assays were run in pairs at an optimum copper concentration (13 μM). Ten microliters of partially purified bovine adrenal DBH was added to duplicate samples as an internal standard to correct for possible variations of activators or inhibitors of DBH (*7*).

Figure 1 shows how DBH activity was distributed along the sural nerve at varying times after ligation. Most striking is the time-dependent increase in DBH activity of the segment immediately proximal to ligature 2. This increase was apparent at 1.5 hours and was dramatic by 5 hours after ligation. Elsewhere along the nerve, changes in DBH activity were minor. After the three longest incubations, there was some increase in DBH activity in the most proximal segment; this could correspond to a small amount of retrograde transport. Inconsistent increases occurred in the DBH activity of the most distal nerve segment.

Total DBH activity per milligram (wet weight) of nerve was unrelated to the time of incubation ($r = -.05$). Since DBH was apparently neither formed nor lost during incubation, the